

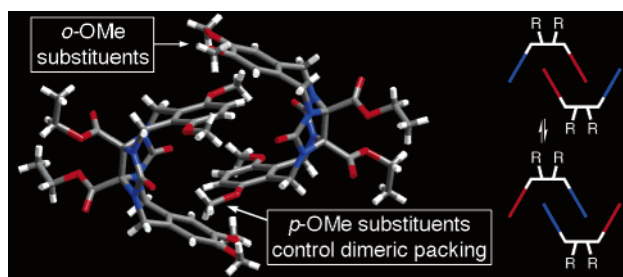
## Substituent Effects Control the Self-Association of Molecular Clips in the Crystalline State

Zhi-Guo Wang,<sup>†</sup> Bao-Han Zhou,<sup>†</sup> Yun-Feng Chen,<sup>†</sup> Guo-Dong Yin,<sup>†</sup> Yi-Tao Li,<sup>†</sup>  
An-Xin Wu,<sup>\*,†</sup> and Lyle Isaacs<sup>\*,‡</sup>

Key Laboratory of Pesticide and Chemical Biology, Ministry of Education, College of Chemistry, Central China Normal University, Wuhan, 430079, PRC, and Department of Chemistry and Biochemistry, University of Maryland, College Park, Maryland 20742

*lisaacs@umd.edu; chwuax@mail.cnu.edu.cn*

Received February 17, 2006



We report the X-ray crystal structure of 11 molecular clips and analyze the influence of substituents (e.g., OMe, Me, and NO<sub>2</sub>) and their location on the observed crystal packing. Molecular clips **3a** and **3b** form tapelike structures in the crystal due to  $\pi$ - $\pi$  interactions between the aromatic walls. Compounds **3d**, **3eC**, and **3fC** form dimers driven by critical C-H $\cdots$ O interactions and then form tapes driven by  $\pi$ - $\pi$  interactions in the crystal. These two building motifs,  $\pi$ - $\pi$  and C-H $\cdots$ O interactions, can be used to rationalize the enantio- and diastereoselectivity observed in the X-ray crystal structures of the remaining five molecular clips. For example, the C-H $\cdots$ O interactions are found to dictate the formation of homochiral dimers in the structures of ( $\pm$ )-**3eT** and ( $\pm$ )-**3fT** and to control the diastereoselective formation of **6a<sub>2</sub>**-**6c<sub>2</sub>** dimeric motifs with internal *p*-dimethoxy-*o*-xylylene walls. Overall, the results suggest that substituent effects that induce even weak intermolecular interactions (e.g., C-H $\cdots$ O) can be used to reliably control crystal packing within glycoluril-based systems.

### Introduction

Glycoluril and its derivatives are now widely used as building blocks for studies of self-assembly in homogeneous solution.<sup>1,2</sup> The resurgence of interest in glycoluril-based supramolecular chemistry can be traced to the work of Mock and co-workers in the 1980s on cucurbit[6]uril (CB[6]).<sup>3</sup> CB[6] is a hexameric glycoluril-based macrocycle with outstanding recognition properties toward organic amines in water.<sup>4</sup> It was the pioneering

work of Rebek and Nolte, however, that made glycoluril commonplace. Rebek's group, for example, studied the H-bond driven self-assembly of glycoluril derivatives into sports-balls in organic solvents and used them to encapsulate guests and promote reactions.<sup>2,5</sup> Of more direct relevance to our studies is the work of Nolte who has pioneered the use of diphenyl glycoluril derived molecular clips in supramolecular chemistry.<sup>1,6</sup> Nolte demonstrated that these diphenyl glycoluril molecular clips have diverse function including acting as receptors for resorcinols,<sup>7</sup> ammonium ions,<sup>8</sup> amino acids,<sup>9</sup> and viologens,<sup>10</sup>

<sup>†</sup> Central China Normal University.

<sup>‡</sup> University of Maryland.

(1) Rowan, A. E.; Elemans, J. A. A. W.; Nolte, R. J. M. *Acc. Chem. Res.* **1999**, *32*, 995–1006.

(2) Hof, F.; Craig, S. L.; Nuckolls, C.; Rebek, J., Jr. *Angew. Chem.* **2002**, *41*, 1488–1508.

(3) Freeman, W. A.; Mock, W. L.; Shih, N. Y. *J. Am. Chem. Soc.* **1981**, *103*, 7367–7368.

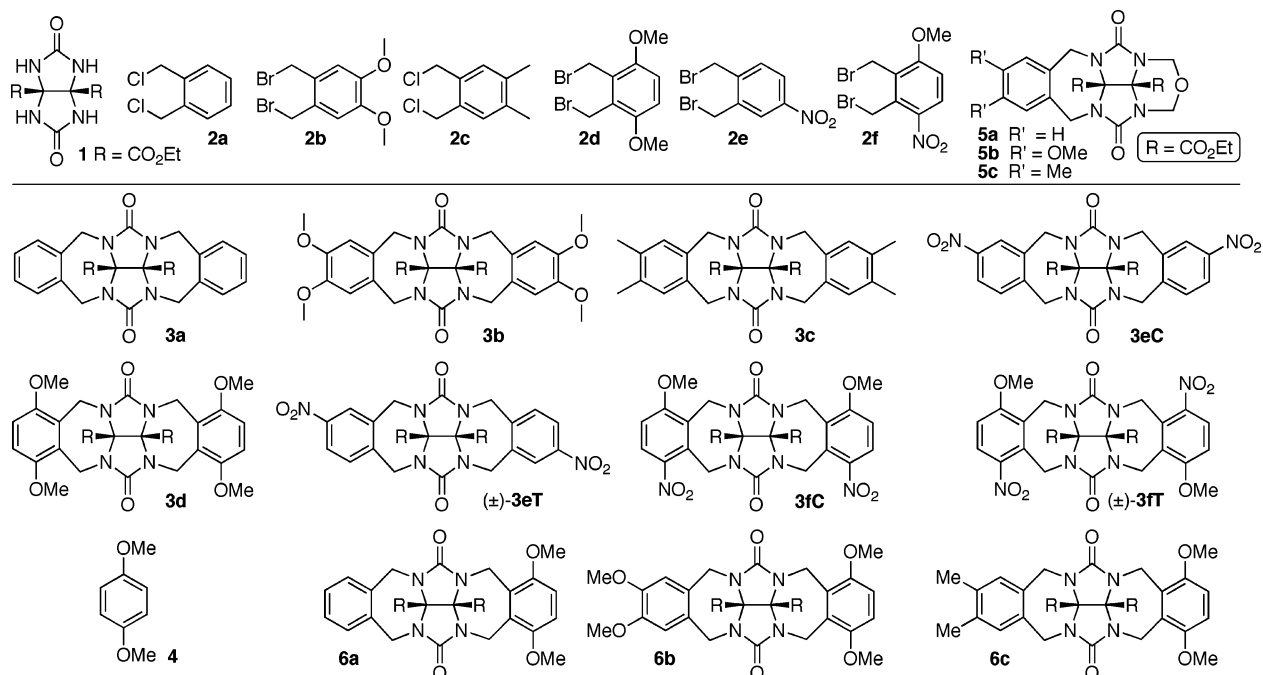
(4) Mock, W. L. *Top. Curr. Chem.* **1995**, *175*, 1–24.

(5) Wyler, R.; de Mendoza, J.; Rebek, J., Jr. *Angew. Chem., Int. Ed. Engl.* **1993**, *32*, 1699–1701. Kang, J.; Rebek, J., Jr. *Nature* **1997**, *385*, 50–52.

(6) Smeets, J. W. H.; Sijbesma, R. P.; Niele, F. G. M.; Spek, A. L.; Smeets, W. J. J.; Nolte, R. J. M. *J. Am. Chem. Soc.* **1987**, *109*, 928–929.

(7) Reek, J. N. H.; Priem, A. H.; Engelkamp, H.; Rowan, A. E.; Elemans, J. A. A. W.; Nolte, R. J. M. *J. Am. Chem. Soc.* **1997**, *119*, 9956–9964.

CHART 1. Compounds Used in This Study



as components of supramolecular vesicles,<sup>11</sup> and as enzyme mimics.<sup>12</sup> More recently, Nolte's group has also studied the self-association of diphenyl glycoluril derived molecular clips in water<sup>13</sup> and organic solvents<sup>1,14</sup> which can be used to build up lamellar thin films.<sup>15</sup>

As part of our interest in the synthetic, mechanistic, and supramolecular chemistry of the cucurbit[*n*]uril family<sup>16</sup> of macrocycles, we had reason to prepare a variety of molecular clips,<sup>17,18</sup> CB[*n*] congeners,<sup>19</sup> CB[*n*] analogues,<sup>20</sup> and new CB[*n*].<sup>21</sup> Along the way, we obtained structural details for a wide variety of compounds by X-ray crystallography. Accordingly, it occurred to us,<sup>22,23</sup> and others,<sup>14,24,25</sup> that glycoluril derivatives might be good building blocks for studies of crystal engineering because of their potential to engage in H-bonding and  $\pi$ - $\pi$  interactions. In this paper, we report the X-ray crystal structures of eleven molecular clips<sup>26</sup> derived from glycoluril **1** which bears two CO<sub>2</sub>Et groups on its convex face and two substituted *o*-xylylene walls. The presence of substituents (e.g., OMe) and their location are found to play a key role in determining the crystal packing because of their ability to engage in C-H $\cdots$ O interactions.

## Results and Discussion

**Selection and Synthesis of Molecular Clips Used in this Study.** Chart 1 shows the structures of glycoluril **1** and bis-(halomethyl) compounds **2a–f** used as starting materials. For the preparation of compounds **3a–f** that contain two identical sidewalls, we performed the alkylation of **1** with the appropriate alkylating agent (**2**) using *t*-BuOK as base in anhydrous DMSO which delivered the target compounds in good yields (30–47%, Supporting Information). The separate alkylation of **1** with **2e** or **2f** delivers two diastereomers that contain two NO<sub>2</sub> groups in a cis (**3eC** and **3fC**) or a trans relationship ( $(\pm)$ -**3eT** and  $(\pm)$ -**3fT**). For the synthesis of molecular clips with two different sidewalls, we performed the electrophilic aromatic substitution reaction between **4** and **5** which gave **6a–c** in excellent yield (>90%). Compounds **3a–f** and **6a–c** contain OMe, NO<sub>2</sub>, and

Me groups on their aromatic rings in a variety of substitution patterns which allows us to assess the influence of substituents on packing in the crystal. By virtue of the substitution pattern,

(8) Smeets, J. W. H.; van Dalen, L.; Kaats-Richter, V. E. M.; Nolte, R. J. M. *J. Org. Chem.* **1990**, *55*, 454–461.

(9) Escuder, B.; Rowan, A. E.; Feiters, M. C.; Nolte, R. J. M. *Tetrahedron* **2004**, *60*, 291–300.

(10) Thordarson, P.; Bijsterveld, E. J. A.; Elemans, J. A. A. W.; Kasák, P.; Nolte, R. J. M.; Rowan, A. E. *J. Am. Chem. Soc.* **2003**, *125*, 1186–1187.

(11) Schenning, A. P. H. J.; Escuder, B.; van Nunen, J. L. M.; de Bruin, B.; Lowik, D. W. P. M.; Rowan, A. E.; van der Gaast, S. J.; Feiters, M. C.; Nolte, R. J. M. *J. Org. Chem.* **2001**, *66*, 1538–1547.

(12) Thordarson, P.; Bijsterveld, E. J. A.; Rowan, A. E.; Nolte, R. J. M. *Nature* **2003**, *424*, 915–918. Schenning, A. P. H. J.; Spelberg, J. H. L.; Hubert, D. H. W.; Feiters, M. C.; Nolte, R. J. M. *Chem.–Eur. J.* **1998**, *4*, 871–880.

(13) Reek, J. N. H.; Kros, A.; Nolte, R. J. M. *Chem. Commun.* **1996**, 245–247. Elemans, J. A. A. W.; Slangen, R. R. J.; Rowan, A. E.; Nolte, R. J. M. *J. Inclusion Phenom. Macrocyclic Chem.* **2001**, *2001*, 65–68. Elemans, J. A. A. W.; Rowan, A. E.; Nolte, R. J. M. *J. Am. Chem. Soc.* **2002**, *124*, 1532–1540. Elemans, J. A. A. W.; Slangen, R. R. J.; Rowan, A. E.; Nolte, R. J. M. *J. Org. Chem.* **2003**, *68*, 9040–9049.

(14) Reek, J. N. H.; Elemans, J. A. A. W.; de Gelder, R.; Beurskens, P. T.; Rowan, A. E.; Nolte, R. J. M. *Tetrahedron* **2003**, *59*, 175–185.

(15) Holder, S. J.; Elemans, J. A. A. W.; Donners, J. J. J. M.; Boerakker, M. J.; de Gelder, R.; Barberá, J.; Rowan, A. E.; Nolte, R. J. M. *J. Org. Chem.* **2001**, *66*, 391–399.

(16) Lagona, J.; Mukhopadhyay, P.; Chakrabarti, S.; Isaacs, L. *Angew. Chem., Int. Ed.* **2005**, *44*, 4844–4870. Lee, J. W.; Samal, S.; Selvapalam, N.; Kim, H.-J.; Kim, K. *Acc. Chem. Res.* **2003**, *36*, 621–630.

(17) Isaacs, L.; Witt, D. *Angew. Chem., Int. Ed.* **2002**, *41*, 1905–1907.

(18) Wu, A.; Chakraborty, A.; Fetting, J. C.; Flowers, R. A., II.; Isaacs, L. *Angew. Chem., Int. Ed.* **2002**, *41*, 4028–4031.

(19) Burnett, C. A.; Witt, D.; Fetting, J. C.; Isaacs, L. *J. Org. Chem.* **2003**, *68*, 6184–6191.

(20) Lagona, J.; Fetting, J. C.; Isaacs, L. *J. Org. Chem.* **2005**, *70*, 10381–10392.

(21) Liu, S.; Zavalij, P. Y.; Isaacs, L. *J. Am. Chem. Soc.* **2005**, *127*, 16798–16799. Isaacs, L.; Park, S.-K.; Liu, S.; Ko, Y. H.; Selvapalam, N.; Kim, Y.; Kim, H.; Zavalij, P. Y.; Kim, G.-H.; Lee, H.-S.; Kim, K. *J. Am. Chem. Soc.* **2005**, *127*, 18000–18001.

(22) Wu, A.; Fetting, J. C.; Isaacs, L. *Tetrahedron* **2002**, *58*, 9769–9777.

(23) Zhou, B. H.; Qu, J. L.; Wu, A. X. *Acta Crystallogr., Sect. E* **2005**, *61*, o3297–o3298.

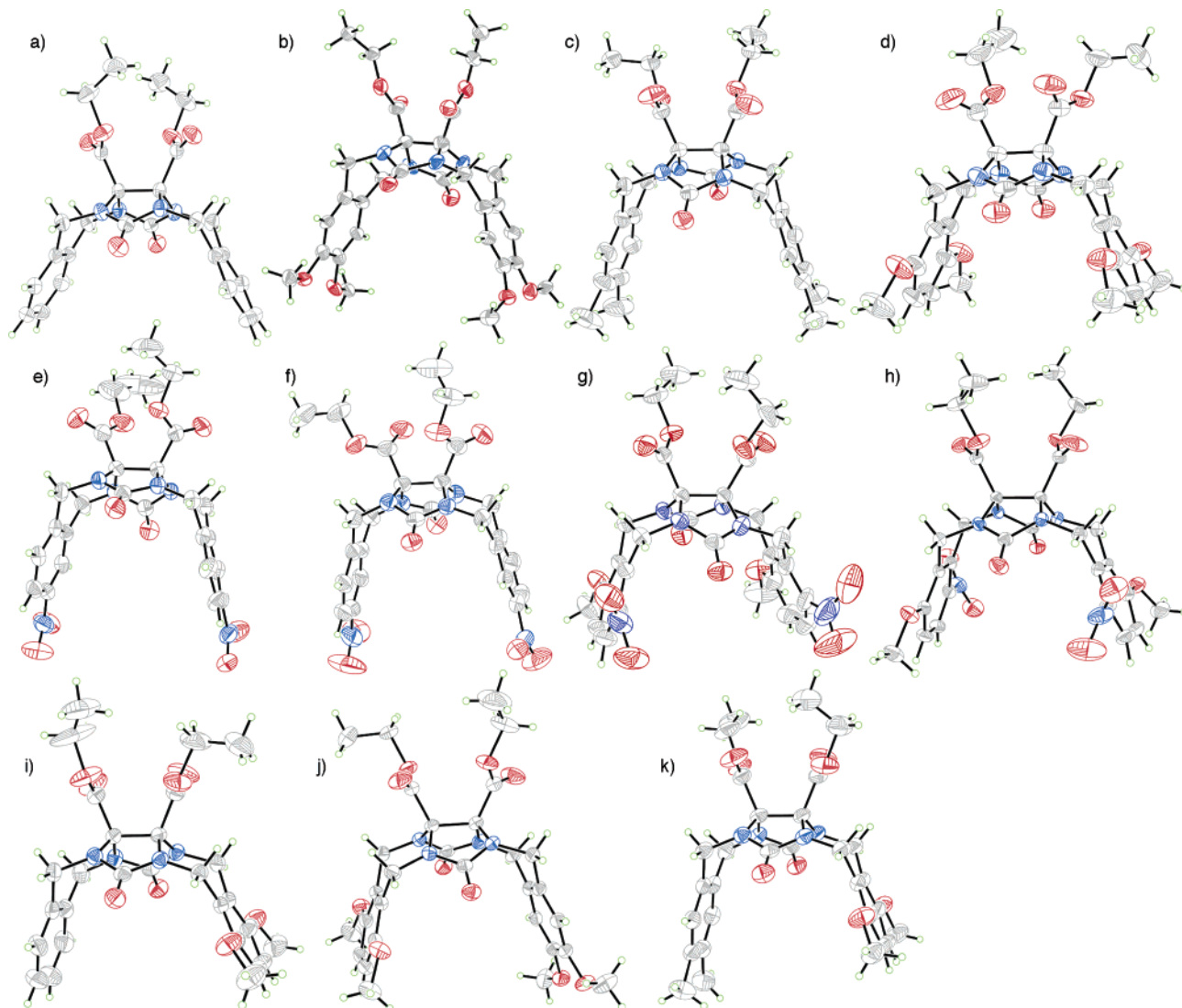


**FIGURE 1.** ORTEP plots of the X-ray crystal structures of: (a) **3a**, (b) **3b**, (c) **3c**, (d) **3d**, (e) **3eC**, (f)  $(\pm)$ -**3eT**, (g) **3fC**, (h)  $(\pm)$ -**3fT**, (i) **6a**, (j) **6b**, (k) **6c**. Color coding: C, gray; H, green; N, blue; O, red.

compounds  $(\pm)$ -**3eT** and  $(\pm)$ -**3fT** with their  $C_2$ -symmetry are chiral but were prepared and used in this study as the corresponding racemic mixture to observe the interplay of substituent effect and chirality. We selected  $\text{CO}_2\text{Et}$ -substituted molecular clips for these studies because they avoid the competing  $\pi$ - $\pi$  stacking motifs possible with Ph-substituted glycoluril-based molecular clips. They also have excellent

solubility in nonpolar organic solvents that do not disturb the packing preferences of the molecular clips by interacting with their ureidyl  $\text{C}=\text{O}$  groups.

#### Molecular Structures of **3a–f** and **6a–c** in the Crystal

We were able to obtain crystals of **3a–f** and **6a–c** that were suitable for X-ray crystal structure determination by slow evaporation of solutions of the various compounds in nonpolar organic solvents ( $\text{CH}_2\text{Cl}_2$ ,  $\text{CHCl}_3$ , and  $\text{CH}_3\text{CN}$ ). Figure 1 shows the molecular structures of **3a–f** and **6a–c** in the crystal. All 11 molecular clips adopt the more commonly observed anti conformation where the substituted *o*-xylylene walls are pointed away from the  $\text{CO}_2\text{Et}$  solubilizing groups on their convex face.<sup>19,27</sup> The geometrical features of these new molecular clips are similar to those reported previously (Table 1).<sup>14,28</sup> For example, the  $=\text{O}\cdots\text{O}=\text{O}$  distances range from 5.49 to 5.65 Å. The distances between the centroids of the substituted *o*-xylylene

(24) Kurth, D. G.; Fromm, K. M.; Lehn, J.-M. *Eur. J. Inorg. Chem.* **2001**, 1523–1526. Johnson, D. W.; Hof, F.; Palmer, L. C.; Martin, T.; Obst, U.; Rebek, J., Jr. *Chem. Commun.* **2003**, 1638–1639. Moon, K.; Chen, W.-Z.; Ren, T.; Kaifer, A. E. *CrystEngComm* **2003**, *5*, 451–453. Kolbel, M.; Menger, F. M. *Chem. Commun.* **2001**, 275–276. Kolbel, M.; Menger, F. M. *Adv. Mater.* **2001**, *13*, 1115–1119. Huo, F.-J.; Yin, C.-X.; Yang, P. *Acta Crystallogr., Sect. C* **2005**, *61*, o500–o502.

(25) Johnson, D. W.; Palmer, L. C.; Hof, F.; Iovine, P. M.; Rebek, J. *Chem. Commun.* **2002**, 2228–2229.

(26) Zimmerman, S. C. *Top. Curr. Chem.* **1993**, *165*, 71–102. Klaerner, F.-G.; Kahlert, B. *Acc. Chem. Res.* **2003**, *36*, 919–932. Harmata, M. *Acc. Chem. Res.* **2004**, *37*, 862–873. Jiang, H.; Leger, J.-M.; Guionneau, P.; Huc, I. *Org. Lett.* **2004**, *6*, 2985–2988. Petitjean, A.; Houry, R. G.; Krytsak, N.; Lehn, J.-M. *J. Am. Chem. Soc.* **2004**, *126*, 6637–6647. Chiang, P.-T.; Cheng, P.-N.; Lin, C.-F.; Liu, Y.-H.; Lai, C.-C.; Peng, S.-M.; Chiu, S.-H. *Chem.–Eur. J.* **2006**, *12*, 865–876. Artacho, J.; Nilsson, P.; Bergquist, K.-E.; Wendt, O. F.; Wärnmark, K. *Chem.–Eur. J.* **2006**, *12*, 2692–2701.

(27) Sijbesma, R. P.; Wijnenga, S. S.; Nolte, R. J. M. *J. Am. Chem. Soc.* **1992**, *114*, 9807–9813.

(28) Reek, J. N. H.; Engelkam, H.; Rowan, A. E.; Elemans, J. A. A. W.; Nolte, R. J. M. *Chem.–Eur. J.* **1998**, *4*, 716–722. Reek, J. N. H.; Rowan, A. E.; Crossley, M. J.; Nolte, R. J. M. *J. Org. Chem.* **1999**, *64*, 6653–6663.

TABLE 1. Selected Parameters from the X-ray Crystal Structures

compound	packing	=O...O= distance (Å)	Ar...Ar centroid distance (Å)	Ar–Ar mean plane angle (°)	$\pi$ – $\pi$ mean plane separation (Å)	solvent
<b>3a</b>	monomer, $\pi$ – $\pi$ tapes	5.617	7.113	56.1	3.69	none
<b>3b</b>	monomer, $\pi$ – $\pi$ tapes	5.501, 5.587	6.560, 6.440	36.2, 37.7	3.58	H <sub>2</sub> O
<b>3c</b>	monomer, no tapes	5.495	6.425	36.2	3.52	CH <sub>3</sub> CN
<b>3d</b>	dimer, non- $\pi$ – $\pi$ tapes	5.647	6.611	42.4	3.46	(ClCH <sub>2</sub> ) <sub>2</sub>
<b>3eC</b>	dimer, $\pi$ – $\pi$ tapes	5.614	6.200	29.6	3.45, 3.53	none
(±)- <b>3eT</b>	homochiral dimer, $\pi$ – $\pi$ tapes	5.653, 5.642	6.145, 6.115	28.0, 27.7	3.36, 3.44	CHCl <sub>3</sub>
<b>3fC</b>	dimer, $\pi$ – $\pi$ tapes	5.535	6.545	38.9	3.52	none
(±)- <b>3fT</b>	homochiral dimer, $\pi$ – $\pi$ tapes	5.485	6.577	37.8	3.47, 3.53	none
<b>6a</b>	dimer, $\pi$ – $\pi$ tapes	5.595	6.620	40.8	3.54	CHCl <sub>3</sub>
<b>6b</b>	dimer, $\pi$ – $\pi$ tapes	5.599	6.332	34.6	3.42	(ClCH <sub>2</sub> ) <sub>2</sub>
<b>6c</b>	dimer, $\pi$ – $\pi$ tapes	5.606	6.280	31.2	3.42	CHCl <sub>3</sub>

rings range from 6.11 to 7.11 Å and depend on the identity of the substituents and their pattern. As the distance between the centroids of the aromatic rings change, so does the angle between the mean planes of these aromatic rings (27.7–56.1°).

**Packing of the Molecular Clips in the Crystal.** Of the eleven compounds examined in this study, eight formed dimeric structures in the crystal by simultaneous penetration of the aromatic sidewalls of two molecular clips into the opposing C-shaped cleft of the type that has been widely explored by Nolte.<sup>1,14,29</sup> In this section, we describe the noncovalent interactions that control the packing of these molecular clips into dimeric entities and their subsequent packing into two- and three-dimensional structures in the crystal.

**A. Packing of Monomeric Molecular Clips in the Crystal.** Compounds **3a–c** remain monomeric in the crystal, although **3b** and **3c** do include solvating H<sub>2</sub>O and CH<sub>3</sub>CN molecules, respectively. An examination of the three-dimensional packing of **3a–c** reveals several recurring structural motifs. Figure 2a shows the tapelike<sup>30</sup> structure that is formed in the crystal structure of **3a**. In this structural motif, the xylylene walls of one molecule of **3a** pack against the identical walls of its neighbors. Although this appears at first glance to be due to direct  $\pi$ – $\pi$  interactions, an examination of the distance between the mean planes of the adjacent aromatic rings (Table 1,  $\pi$ – $\pi$  mean plane separation: 3.69 Å) suggests this motif also results from dispersive interactions between the CH<sub>2</sub> groups and the adjacent Ar ring. A related tapelike packing motif occurs in the X-ray crystal structures of monomeric **3b** (Figure 2b), although the separation between the mean planes of the Ar rings for **3b** is smaller (3.58 Å). An examination of the packing of the tapelike structures of **3a** and **3b** reveals that they are held together by a second type of packing motif based on C–H...O interactions between polarized C–H bonds and the ureidyl carbonyl groups of an adjacent molecular clip (Table 2). In the structure of **3a**, this manifests itself as a pairwise interaction between both CO<sub>2</sub>Et groups of one molecular clip and the cleft of the adjacent clip, whereas for **3b**, an OMe group on **3b** packs against the ureidyl carbonyl group on an adjacent molecule of **3b**. The structure of **3c** (Figure 2c) is quite different from those of **3a** and **3b** as a result of the solvating CH<sub>3</sub>CN molecules that fill the clefts of **3c**. Quite interestingly, the substituted *o*-xylylene

walls of two adjacent molecules of **3c** shape a molecular box around the cavity of **3c**·CH<sub>3</sub>CN that resembles a calixarene-type receptor. The structure of **3c** also displays close contacts between the CO<sub>2</sub>Et groups of 1 equiv of **3c** and an adjacent molecule of **3c** in the crystal. The two recurring packing motifs, Ar–Ar interactions between the sidewalls of molecular clips and close contacts between polarized C–H bonds and the ureidyl C=O groups of adjacent molecular clips, will be used below to rationalize the buildup of three-dimensional packing of dimeric molecular clips in the crystal.

**B. Dimeric Packing of Achiral Molecular Clips 3d, 3eC, and 3fC in the Crystal.** Aside from **3a–c**, the remaining molecular clips **3d–f** and **6a–c** all form dimeric structures in the crystal. Similar to the monomeric clips **3a–c**, we have found

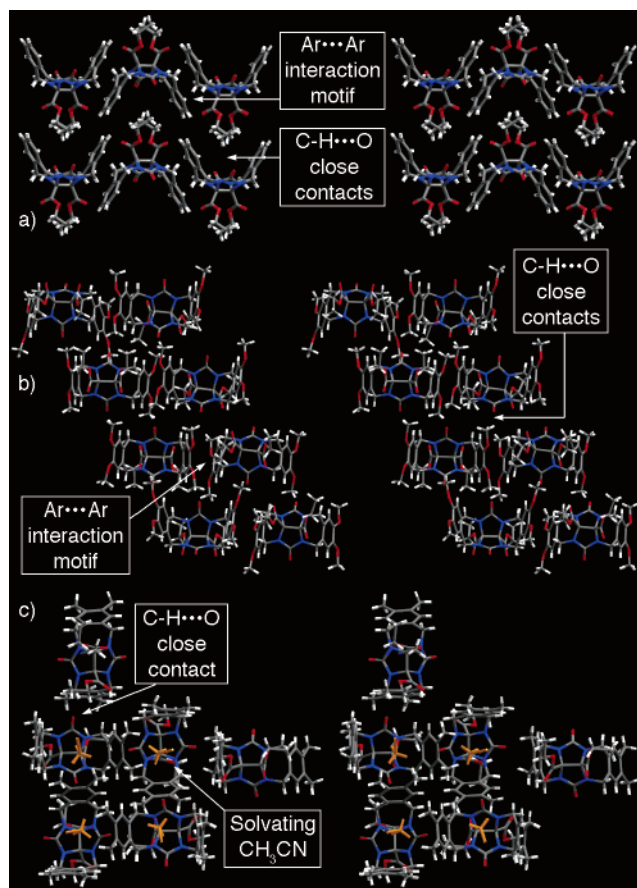


FIGURE 2. Cross-eyed stereoviews of the packing motifs observed for: (a) **3a**, (b) **3b**, and (c) **3c**. Color coding: C, gray; H, white; N, blue; O, red; solvating CH<sub>3</sub>CN, orange.

(29) (a) Reek, J. N. H.; Rowan, A. E.; de Gelder, R.; Beurskens, P. T.; Crossley, M. J.; de Feyter, S.; de Schryver, F.; Nolte, R. J. M. *Angew. Chem., Int. Ed. Engl.* **1997**, *36*, 361–363. (b) Holder, S. J.; Elemans, J. A. A. W.; Barberá, J.; Rowan, A. E.; Nolte, R. J. M. *Chem. Commun.* **2000**, 355–356.

(30) MacDonald, J. C.; Whitesides, G. M. *Chem. Rev.* **1994**, *94*, 2383–2420. Meléndez, R. E.; Hamilton, A. D. *Top. Curr. Chem.* **1998**, *198*, 97–129.

**TABLE 2.** Parameters from Selected C–H···O Interactions Observed in the Crystal Structures

compound	C···O distance (Å)	H···O distance (Å)	C–H···O angle (°)
<b>3a</b>	3.73	2.89	147.4
<b>3b</b>	3.24	2.47	136.9
<b>3c</b>	3.17	2.60	117.5
<b>3d</b>	3.33, 3.19	2.76, 2.50	118.4, 128.8
<b>3eC<sup>a</sup></b>	–	–	–
<b>(±)-3eT</b>	3.34, 3.38	2.44, 2.48	164.1, 162.8
<b>3fC</b>	3.49	2.72	138.2
<b>(±)-3fT</b>	3.31	2.60	130.5
<b>6a</b>	3.46, 3.46	2.61, 2.73	148.8, 134.1
<b>6b</b>	3.51, 3.20	2.82, 2.54	129.9, 125.9
<b>6c</b>	3.51, 3.31	2.83, 2.63	128.5, 128.2

<sup>a</sup> – = no C–H···O contacts to the ureidyl C=O group.

that interactions between the aromatic rings and packing of polarized C–H groups against the ureidyl C=O group of the glycoluril play a decisive role in the buildup of the three-dimensional structure of crystalline **3d–f** and **6a–c**. In this section, we examine the crystal structures of **3d**, **3eC**, and **3fC** which are achiral and contain two identical aromatic walls.

Figure 3a illustrates the dimeric packing motif observed for **3d**. The first striking feature of the structure of **3d** is the coplanarity of the two *internal* aromatic rings. The mean planes of these aromatic rings are separated by 3.46 Å indicating that these aromatic rings benefit from direct  $\pi$ – $\pi$  interactions in the crystal.<sup>31</sup> The remaining pairs (e.g., internal/external) of aromatic rings are tilted with respect to one another and do not benefit from direct  $\pi$ – $\pi$  interactions in the dimer. Why does compound **3d** form dimers in the crystal whereas **3a–c** do not? On the basis of an examination of **3d** and the structures of the other dimeric molecular clips (vide infra), we suggest that the presence of close contacts between the polarized C–H bonds of the OCH<sub>3</sub> substituents on **3d** with the ureidyl C=O groups on the opposing equivalent of **3d** play an important role. Because the distance between the *p*-OMe groups does not match the glycoluril C=O···O=C distance, there are two crystallographically independent sets of contacts. For **3d**, the shorter (longer) C···O contact is 3.191 Å (3.329 Å) and the shortest C–H···O contact amounts to 2.501 Å (2.764 Å). Such distances are comparable to the sum of the corresponding van der Waals radii (3.4 Å) which suggests the presence of C–H···O interactions (Table 2) for crystalline **3d**.<sup>32</sup> The dimeric unit of **3d** repeats along the crystallographic *b*-axis which leads to tapelike structures (Figure 3a).

Figure 3b shows the crystal packing observed for **3eC**. The dimerization of **3eC** benefits from  $\pi$ – $\pi$  interactions between the coplanar internal aromatic rings whose mean planes are separated by 3.45 Å. Because of the placement of the NO<sub>2</sub> groups, **3eC** could adopt either head-to-head or head-to-tail arrangements within dimeric **3eC**<sub>2</sub>. In the crystal, **3eC** exclusively adopts the centrosymmetric head-to-tail arrangement (e.g., two NO<sub>2</sub> groups up, two down) presumably so that the NO<sub>2</sub> dipoles cancel each other. The dimeric units **3eC**<sub>2</sub> pack along the *ab*-axis because of  $\pi$ – $\pi$  interactions between their external aromatic rings (mean plane separation = 3.53 Å) to form tapelike structures. The tapes pack along the *c*-axis because of

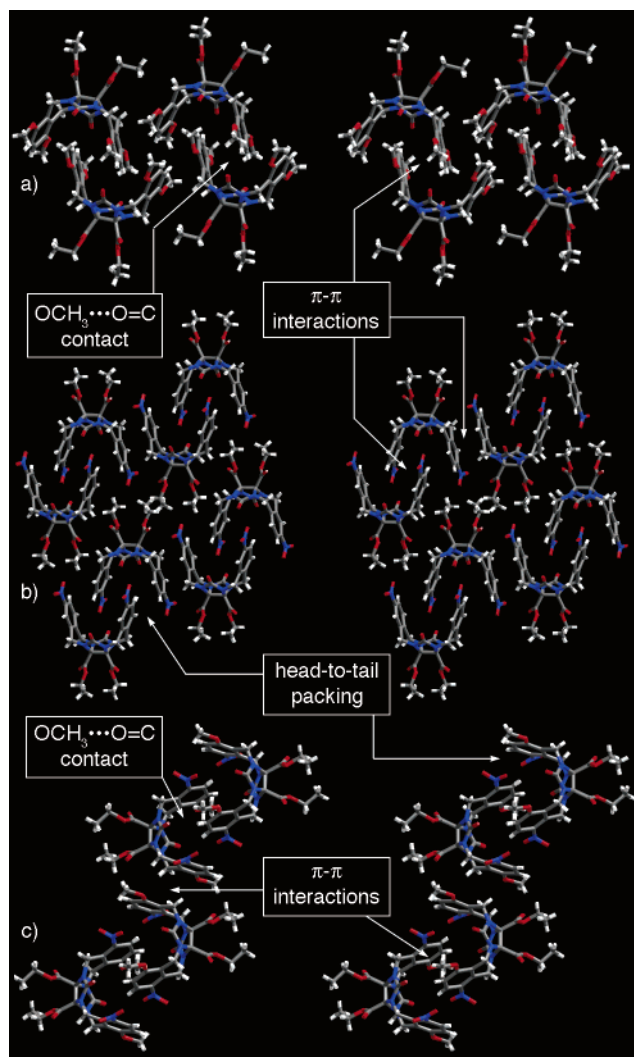


**FIGURE 3.** Cross-eyed stereoviews of the dimeric packing motifs observed for achiral: (a) **3d**, (b) **3eC**, and (c) **3fC**. Color coding: C, gray; H, white; N, blue; O, red.

an interdigitation of the CO<sub>2</sub>Et groups on the convex face of the constituent **3eC**. Figure 3c illustrates the crystal packing of **3fC**. Similar to **3d** and **3eC**, **3fC** assumes a dimeric arrangement in the crystal such that the two internal aromatic rings are coplanar with a mean plane separation (3.52 Å) near the preferred offset  $\pi$ – $\pi$  stacking distance.<sup>33</sup> Within these dimeric units, there are two symmetry equivalent C–H···O close contacts (C···O = 3.49) between the OCH<sub>3</sub> and ureidyl C=O groups. The external aromatic rings of the dimers form an offset  $\pi$ – $\pi$  stack with a mean plane separation of 3.54 Å along the *c*-axis leading to tapelike structures. These tapes further pack with interdigitation of their CO<sub>2</sub>Et groups. In combination, the structures of monomeric clips **3a–c** and dimers of achiral clips **3d**, **3eC**, and **3fC** suggest that  $\pi$ – $\pi$  interactions between the internal and external pairs of aromatic rings along with C–H···O close contacts control the arrangement of molecular clips in the crystal.

**C. Dimeric Packing of Chiral Molecular Clips (±)-3eT and (±)-3fT in the Crystal.** On the basis of the packing motifs

(31) A similar geometry has previously been observed by Nolte for diphenylglycoluril-based molecular clips (refs 14 and 29).

(32) Taylor, R.; Kennard, O. *J. Am. Chem. Soc.* **1982**, *104*, 5063–5070. Desiraju, G. R. *Acc. Chem. Res.* **1991**, *24*, 290–296. Seiler, P.; Isaacs, L.; Diederich, F. *Helv. Chim. Acta* **1996**, *79*, 1047–1058.

(33) Waters, M. L. *Curr. Opin. Chem. Biol.* **2002**, *6*, 736–741.

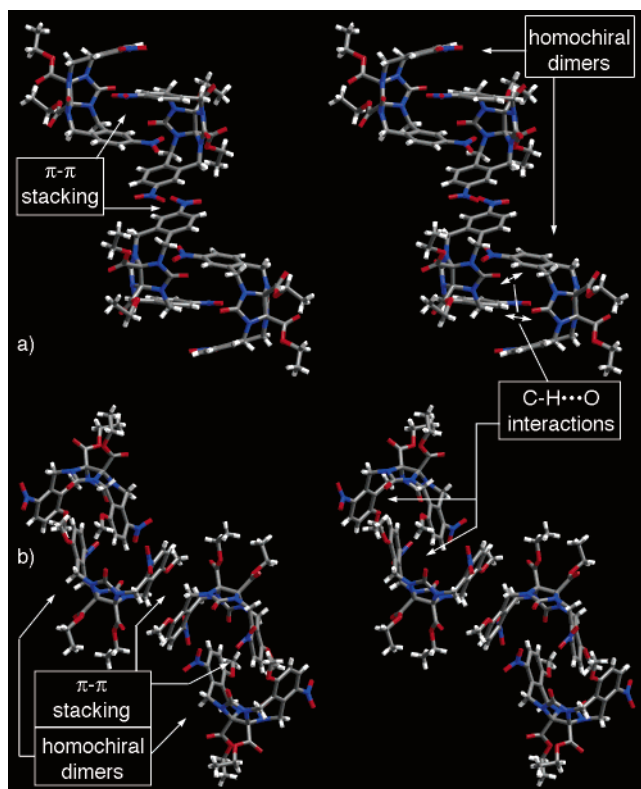
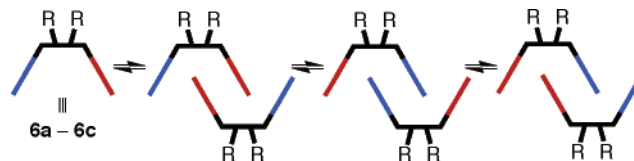


**FIGURE 4.** Cross-eyed stereoviews of the dimeric packing motifs observed for racemates: (a)  $(\pm)$ -**3eT** and (b)  $(\pm)$ -**3fT**. Color coding: C, gray; H, white; N, blue; O, red.

observed for the monomeric and achiral dimeric clips (vide supra), we wondered whether it would be possible to understand the structures of their chiral counterparts ( $(\pm)$ -**3eT** and  $(\pm)$ -**3fT**). Figure 4a shows the crystal structure of  $(\pm)$ -**3eT**. Just as in the case of **3eC**,  $(\pm)$ -**3eT** undergoes dimerization in the crystal driven by  $\pi$ - $\pi$  stacking interactions; the Ar rings are not coplanar with a mean-plane separation of 3.36 Å (range: 3.13–3.61 Å). Interestingly, the two enantiomers  $(+)$ -**3eT** and  $(-)$ -**3eT** undergo enantiomeric self-recognition<sup>17,34</sup> during crystallization to form the homochiral dimers  $(+)$ -**3eT**<sub>2</sub> and  $(-)$ -**3eT**<sub>2</sub> driven most likely by the presence of a C–H $\cdots$ O H-bond between the proton ortho to the NO<sub>2</sub> group and the ureidyl C=O group on the glycoluril skeleton. In the homochiral dimeric pairs, two weak C–H $\cdots$ O H-bonds are possible, whereas for the hypothetical heterochiral pair,<sup>18</sup> only a single C–H $\cdots$ O H-bond could be formed which provides the driving force for the observed enantiomeric self-recognition. Despite the fact that  $(\pm)$ -**3eT** undergoes enantiomeric self-recognition, this is not an example of conglomerate formation because the two homochiral pairs  $(+)$ -**3eT**<sub>2</sub> and  $(-)$ -**3eT**<sub>2</sub> alternate with one another in the crystal. Figure 4a illustrates how the homochiral pairs interact with one another by  $\pi$ - $\pi$  interactions between their external aromatic rings to form tapelike motifs along the *c*-axis. Interestingly, the tapes pack with their long axes parallel and in register, that is, dimers of the same handedness are segregated into sheets in the *ab*-plane that alternate in their sense of chirality. An unusual feature of the homochiral dimers of **3eT**

**SCHEME 1.** Illustration of the Three Different Dimeric Packing Motifs that Are Possible for **6a–c** that Contain Two Different Substituted *o*-Xylylene Walls



is that, rather than being in parallel register with one another, the constituent monomers are twisted by 90° apparently to satisfy the C–H $\cdots$ O H-bond geometrical preference. Compound  $(\pm)$ -**3fT** also forms a dimeric motif in the crystal due in part to  $\pi$ - $\pi$  interactions between the substituted *o*-xylylene walls (mean plane separation: 3.47 Å). In addition, the dimeric building block motif benefits from OCH<sub>3</sub> $\cdots$ O interactions (C $\cdots$ O = 3.308 Å). We rationalize that the simultaneous formation of two such C–H $\cdots$ O interactions in the homochiral form drives the observed enantiomeric self-recognition process because the hypothetical heterochiral form would only benefit from a single good C–H $\cdots$ O interaction. Similar to  $(\pm)$ -**3eT**, the homochiral dimers  $(+)$ -**3fT**<sub>2</sub> and  $(-)$ -**3fT**<sub>2</sub> alternate along the crystallographic *c*-axis forming tapelike structures that benefit from  $\pi$ - $\pi$  interactions between their external aromatic rings (mean plane separation: 3.53 Å). Once again, the tapes pack with their long axes parallel and segregate the homochiral dimers into alternating homochiral slabs along the *ab*-plane. Although the crystal structures of  $(\pm)$ -**3eT** and  $(\pm)$ -**3fT** contain many features seen in the structures described above (e.g., internal and external  $\pi$ - $\pi$  interactions and C–H $\cdots$ O interactions), other features are new (e.g., efficient homochiral dimerization and segregation in homochiral planes) which suggests the broad potential of glycoluril derivatives in crystal engineering studies.

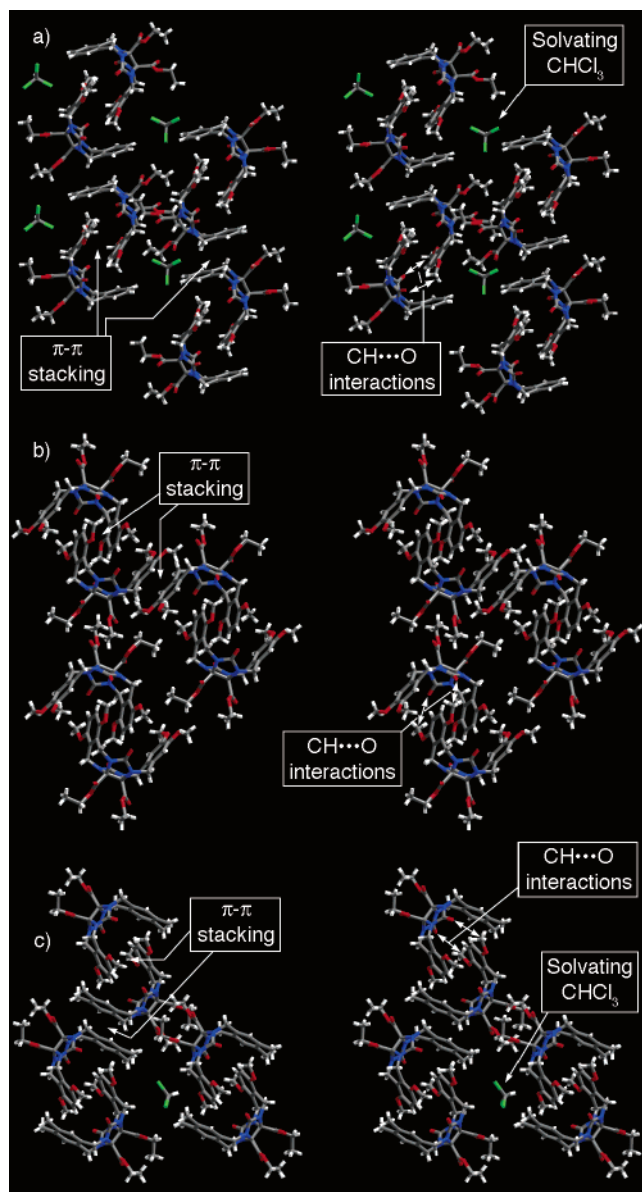
**D. Dimeric Packing of Achiral Molecular Clips Containing Two Different Aromatic Walls in the Crystal.** On the basis of the results described above which indicate that OCH<sub>3</sub> $\cdots$ O=C interactions and  $\pi$ - $\pi$  stacking control the dimerization and packing of molecular clips containing two identical aromatic walls, we wondered whether it would be possible to control diastereoselectivity during crystallization of molecular clips containing two different aromatic walls. For example, when two such molecular clips dimerize, three diastereomers are possible: two isomers with identical walls (e.g., red or blue) in the interior of the dimer and a third with one of each type of aromatic wall in the interior (Scheme 1).<sup>35</sup> To investigate this type of isomerism, we prepared compounds **6a–c** which each contain one *p*-dimethoxy-*o*-xylylene wall. We predicted that this wall with its capacity for both  $\pi$ - $\pi$  and C–H $\cdots$ O interactions would control the diastereomer selection during crystallization.

Figure 5 shows the X-ray crystal structures obtained for **6a–c** which indicates that this prediction is valid. For example, Figure 5a shows the structure of **6a** in the crystal. Compound **6a** once again packs as dimers in the crystal because of  $\pi$ - $\pi$  interactions (mean plane separation = 3.54 Å). During this dimerization, both *p*-dimethoxy-*o*-xylylene rings are positioned in the interior of the dimer, contrary to what might be expected based on the electrostatic potentials of the aromatic rings<sup>33,36</sup> but perfectly

(34) Shi, X.; Fettinger, J. C.; Davis, J. T. *J. Am. Chem. Soc.* **2001**, *123*, 6738–6739. Ishida, Y.; Aida, T. *J. Am. Chem. Soc.* **2002**, *124*, 14017–14019. Murguly, E.; McDonald, R.; Branda, N. R. *Org. Lett.* **2000**, *2*, 3169–3172.

(35) The X-ray crystal structure of a porphyrin-derived molecular clip (ref 29a) displays a similar preference for internal *p*-dimethoxy-*o*-xylylene walls.

(36) Cozzi, F.; Cinquini, M.; Annuziata, R.; Siegel, J. S. *J. Am. Chem. Soc.* **1993**, *115*, 5330–5331.



**FIGURE 5.** Cross-eyed stereoviews of the dimeric packing motifs observed for: (a) **6a**, (b) **6b**, and (c) **6c**. Color coding: C, gray; H, white; N, blue; O, red.

in line with the prediction that C–H···O interactions will control diastereomer selection. For **6a<sub>2</sub>**, two different sets of C–H···O interactions are present with short C···O distances (both 3.46 Å, Table 2). Once again, these dimers pack into tapelike structures because of weak external Ar–Ar interactions (mean plane separation = 3.65 Å) along the *b*-axis. The three-dimensional packing of **6a** is similar to that observed for the other clips, with interdigitation of the CO<sub>2</sub>Et groups. For **6a**, however, solvating CHCl<sub>3</sub> appears to play the role of filling space that would otherwise be left unfilled because of the absence of substituents on one aromatic wall. Compound **6b** with an *o*-dimethoxy-*o*-xylylene wall crystallizes following a similar set of rules. Dimerization of **6b** with internal *p*-dimethoxy-*o*-xylylene walls is driven by  $\pi$ – $\pi$  interactions (mean plane separation = 3.42 Å) and OCH<sub>3</sub>···O=C interactions (C···O = 3.20; 3.51 Å). Tapes (Figure 5b) are formed by external  $\pi$ – $\pi$  interactions (mean plane separation = 3.30 Å) and subsequently pack with their long axes parallel along the

*b*-axis. The X-ray structure of **6c**, with its *o*-dimethyl-*o*-xylylene walls, is analogous to **6a**. Dimerization is mediated by internal  $\pi$ – $\pi$  interactions between the two *p*-dimethoxy-*o*-xylylene walls (mean plane separation = 3.42 Å) and OCH<sub>3</sub>···O=C interactions (C···O = 3.31, 3.51 Å). External  $\pi$ – $\pi$  interactions holding the tapes together appear to be weak (mean plane separation = 3.59 Å). The tapes align parallel to one another along the *ab*-diagonal while including solvating CHCl<sub>3</sub> molecules.

## Conclusions

We have presented the X-ray crystal structures of eight glycoluril-based molecular clips bearing different substituents (e.g., H, OMe, NO<sub>2</sub>, and Me) on their aromatic rings and different substitution patterns, some of which are chiral. We have also presented the crystal structures of three glycoluril-derived molecular clips that bear two differentially substituted walls. Compounds **3a–c** that lack a *p*-methoxy substituent are monomeric in the crystal structure. The remaining compounds exhibit dimeric molecular clips as building motifs in the crystal. We attribute this result to the simultaneous formation of OCH<sub>3</sub>···O=C interactions and  $\pi$ – $\pi$  stacking between the internal aromatic rings. The interplay between the  $\pi$ – $\pi$  interactions and C–H···O interactions in the solid-state structures of ( $\pm$ )-**3eT** and ( $\pm$ )-**3fT** results in high levels of enantioselectivity during the exclusive formation of homochiral dimeric motifs. Similar considerations also control diastereoselectivity in the solid-state structures of **6a–c** with their *p*-dimethoxy-*o*-xylylene rings in the interior of the dimeric molecular clips.

Although the supramolecular chemistry of glycoluril-based systems in a homogeneous solution is well established, the use of glycoluril derivatives as building blocks for crystal engineering studies has only recently begun to be explored.<sup>14,22,25</sup> Both we and Rebek have previously used the H-bonding potential of glycoluril itself to engineer the formation of H-bonded tapes in the crystal. In this paper, we established that even weaker, less directional noncovalent interactions (e.g.,  $\pi$ – $\pi$  interactions and C–H···O interactions) can be used to reliably and predictably build up complex crystalline architectures. In combination, these results suggest that the potential of glycoluril derivatives in studies of crystal engineering may be as broad as has been demonstrated for its solution chemistry.

**Acknowledgment.** We thank Central China Normal University, National Natural Science Foundation (No. 20472022), Hubei Province Natural Science Fund (Nos. 2004ABA085 and 2004ABC002), University of Maryland, and the NIH (GM61854) for generous financial support. We thank Xiang-Gao Meng for performing the X-ray crystallographic measurements.

**Supporting Information Available:** General experimental, synthetic procedures and characterization data, selected <sup>1</sup>H and <sup>13</sup>C NMR spectra for all new compounds (pdf), and crystallographic information files (cif). This material is available free of charge via the Internet at <http://pubs.acs.org>.

JO0603375